JMEPEG (2007) 16:470–476
DOI: 10.1007/s11665-007-9070-y

1059-9495/$19.00

Processing and Mechanical Properties of Natural Rubber-$ZnFe_2O_4$ Nanocomposites

C. Piña-Hernández, L. Hernández, L. M. Flores-Vélez, L. F. del Castillo, and O. Domínguez

(Submitted April 18, 2006; in revised form August 23, 2006)

We present preliminary results concerning natural rubber reinforced with nanometric $ZnFe_2O_4$ obtained from an industrial solid waste. The study investigate the influence of these nanometric ceramic particles on the processing as well as the mechanical properties of the obtained rubber composite, opening the possibility of partial replacement of carbon black and exposing a new potential composite material. The hardness of unfilled and reinforced rubber increased as nanometric $ZnFe_2O_4$ was increased. Besides, tensile properties of the reinforced rubber were measured, observing once again that as the amount of nanometric $ZnFe_2O_4$ particles was increased, ultimate strength improved from 2.5 MPa to almost 20 MPa.

Keywords mechanical properties, nanocomposites, natural rubber, vulcanization

1. Introduction

The purpose of adding mineral fillers to polymers was primarily one to improve mechanical properties and to get cost reduction. However, in recent years the fillers are more often used to fulfill a functional role, such as increasing the stiffness or improve the dimension stability of the polymer (Ref 1). The mineral fillers used in polymers are usually kaolin, talc, silica, and calcium carbonate and, to a lesser extend mica and wollastonite (Ref 2).

Carbon black is unquestionably the most widely used reinforcing filler in elastomer formulations, owing to the physicochemical characteristics and performances it gives to cured rubbers (Ref 3). However, instability of the price of petroleum could result in a growing interest for other mineral fillers, such as precipitated calcium carbonate, silica (Ref 4, 5) and in the present case, $ZnFe_2O_4$ nanometric particles obtained from industrial solid wastes. Wagner (Ref 6, 7) reviewed the use of precipitated silica and silicates in rubber, showing that with the addition of these ingredients, better properties were provided, including resistance to tear, hardness, stiffness, and high resilience. Nevertheless, the use of precipitated silica brings higher costs, sometimes forbidding its use in some formulations, which therefore must be compounded with other mineral fillers, like clays, chalks, or carbonates, usually leading to inferior technological performance.

It is well known that the mechanical properties of crosslinked rubber systems are enhanced by the incorporation of particulate fillers, such as carbon black and silica (Ref 6-9). Further, such reinforcements are related to the secondary structure of filler particles (agglomerate) (Ref 10-11) and it is generally accepted that the tensile stress at relatively large strains (>100%) is closely related to the extent of the rubber/filler interaction (Ref 12, 13).

At present, one of the major by-products of steel-making industry is the electric-arc-furnace dust (EAFD), where thousands of tons of dust are generated in steel-smelting plants each year. Because of the extremely fine particles of the powders, principally in the nanometric domain, one of the possible applications of EAFD could be as reinforcing particles in rubbers.

The present work exposes preliminary results concerning EAFD-reinforced natural rubber. The study investigate the influence of these nanometric ceramic particles on the vulcanization as well as the mechanical properties of the obtained rubber, opening the possibility of partial replacement of carbon black and exposing a new potential composite material.

2. Experimental

2.1 Sample Preparation and Processing

Technically specified natural rubber of grade 5 used as base elastomer was supplied by a domestic company ($M_w = 5.4 \times 10^5$ g/mole). Domestic EAFD and fly-ash (FA) were used as fillers and no coupling agents were added for the surface modification of these particles. EAFD is formed basically of nanometric particles and FA is constituted of micrometric particles so it was used to compare the behavior of the nanometric EAFD particles when added in natural rubber.

It was selected a conventional sulfur cure system resulting in predominantly polysulfidic crosslinks at optimum cure (Ref 2). The chemical composition of the compounded natural rubber (CNR) is shown in Table 1. Various kinds of composites were prepared by mechanical mixing the CNR with the selected fillers, naming NC and MC to those achieved with nanometric

C. Piña-Hernández, L. Hernández, and **O. Domínguez,** Instituto de Metalurgia, UASLP, 550 Sierra Leona, CP 78210 San Luis Potosi, SLP, Mexico; **L. M. Flores-Vélez,** Facultad de Química, UASLP, 6 Av. Nava, CP 78210 San Luis Potosi, SLP, Mexico; and **L. F. del Castillo,** Instituto de Materiales, UNAM, Circuito Exterior s/n, CP 03025 Mexico City, Mexico. Contact e-mail: nanoquimica@yahoo.com.

Table 1 Chemical composition of the compounded natural rubber

	Natural rubber	Sulfur	Zinc oxide	Stearic acid	TMTD[a]	MBT[b]	Paraffinic oil
Wt.%	88.56	1.98	4.43	1.35	1.55	0.65	1.48

[a]TMTD: tetramethylthiuram disulfide
[b]MBT: 2-mercaptobenzothiazole

and micrometric particles obtained from EAFD and FA, respectively, their composition being listed in Table 2.

The mixing and compounding of natural rubber with fillers and additives was carried out in a laboratory two-roll mill at 55 °C, following the conventional technique. Figure 1 corresponds to the unvulcanized materials obtained after roll milling the natural rubber with the corresponding fillers and additives, where CNR correspond to natural rubber processed with only the vulcanizing agents shown in Table 1, CM was processed using CNR and FA, and CN correspond to the material obtained after processing CNR with EAFD. From Fig. 1, it is palpable that the final color of the composite strongly depends on the filler added to the rubber.

2.2 Vulcanization Procedure

The vulcanization behavior of raw FA and EAFD blends was determined on a Monsanto Rheometer using a 3° rotor oscillation amplitude and frequency of 1.67 Hz at an isothermal temperature of 160 °C. Cylindrical compounded wafers were compression molded under a pressure of 4 MPa at 160 °C. An optimum cure time of 8 min for molding was estimated from torque-time curves given by rheometry and from these wafers, vulcanized slabs were obtained for mechanical testing.

2.3 XRD and Mechanical Properties

X-ray diffraction (XRD) experiments were performed employing a diffractometer with Cu K_α radiation and a nickel monochromator, using a scanning speed of 0.01°/min and an integration time of 2 s over the range 2θ from 10° to 80°. Measurements of stress-strain curves were carried out at room temperature under displacement control, using an universal testing machine with capacity of 10,000 kg and a crosshead speed of 0.76 mm/min was used.

2.4 Transmission and Scanning Electron Microscopy

Scanning electron microscopy (SEM) observations were carried out on fractured surfaces of the vulcanized slabs. The SEM micrographs were taken under an accelerating voltage of 15 kV. Transmission electron microscopy (TEM) observations were carried out on nanometric EAFD using an accelerating voltage of 120 kV. Chemical microanalysis was performed by energy dispersive spectrometry (EDS) attached to electron microscopes.

Fig. 1 Photograph showing unvulcanized materials after roll-mill processing. CNR: compounded natural rubber; MC: CNR + FA and NC: CNR + EAFD

3. Results and Discussion

3.1 Materials Characterization

Energy dispersive spectrometry and XRD were used to determine the chemical composition of the EAFD. Figure 2 shows that EAFD was basically determined as $ZnFe_2O_4$ with smaller amounts ZnO and hematite Fe_2O_3. EDS analysis carried out on EAFD indicated the presence of small amounts of Pb and Mn in the particles (Table 3).

The size, distribution, and shape of the EAFD particles were evaluated using TEM images (Fig. 3). The EAFD was mainly composed of nanometric particles presenting filamentary (*t*), faceted (*c*) and spherical shape (*s*), with a mean particle size of about 120 nm (Fig. 3). Besides, TEM images indicated that particles are agglomerated forming bigger clusters, with a mean size ranging from 400 to 800 nm. Chemical composition of domestic FA is indicated on Table 3. X-ray diffraction was used to determine the chemical phases present on FA. Figure 4 shows that FA was basically determined as $Al_6Si_2O_{13}$ and SiO_2. The size distribution and shape of FA particles was evaluated

Table 2 Composition of natural rubber composites

	CNR (wt.%)	EAFD (wt.%)	EAFD (vol.%)		CNR (wt.%)	FA (wt.%)	FA (vol.%)
NR	100	0	0	NR	100	0	0
NC30	70	30	9.47	MC30	70	30	15.25
NC40	60	40	13.57	MC40	60	40	21.26
NC50	50	50	17.31	MC50	50	50	26.47

using SEM images (Fig. 5), finding a mean particle size of 25 μm. Besides, pycnometric measurements carried out on FA and EAFD indicated a mean apparent density of 2.5 and 4.3 g/cm^3, respectively.

3.2 Rheological Properties

Torque-time curves given by torque rheometry at 160 °C are shown in Fig. 6a and b. Diminution of torque values, due to material loading and a stable plateau region in the later stage of vulcanization process, were observed during the rheological evaluation of all the blends. When the cross-linking process starts, a sharp increase in torque was observed after several minutes. The maximum torque values were a clear indication that the vulcanization reaction had taken place in the blend, and for the present formulation the vulcanization process takes about 7 min.

Although MC and NC blends were compounded with fillers having extremely different particle sizes, the final torque was equivalent as could be seen in Fig. 6. Crosslinking was slightly sooner in the micrometric powders as could be observed from their sharp torque increase at lower times, whereas the nanometric powders had the tendency to vulcanize at higher times. Stearic acid and zinc oxide are accepted throughout the rubber industry as being adequate for achievement of optimum vulcanization with a wide range of accelerator to sulfur ratios (Ref 1, 2). Nevertheless, work concerning the electronegativity of several metals of the oxides evaluated vs. rheometer torque has indicated that outside a given electronegativity range of 1.6-1.8 (Ref 5), the presence of metallic ions other than Zn could modify vulcanization. Consequently, the different vulcanization behavior observed between nanometric and micrometric particles probably comes from the presence of some electronegative metals in the powders.

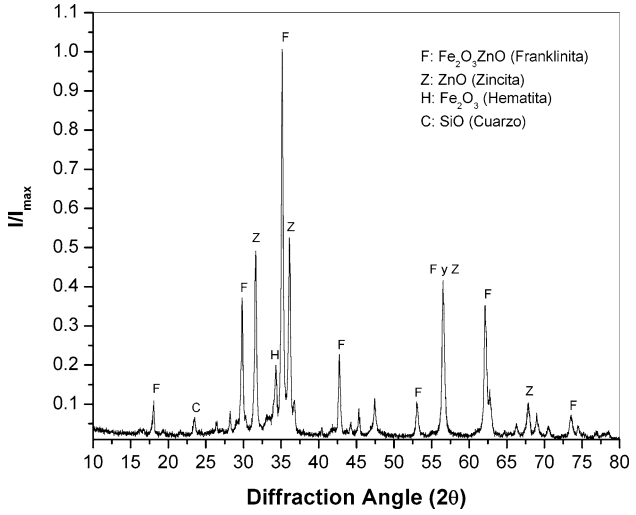

Fig. 2 X-ray diffraction pattern obtained from the electric-arc-furnace dust (EAFD)

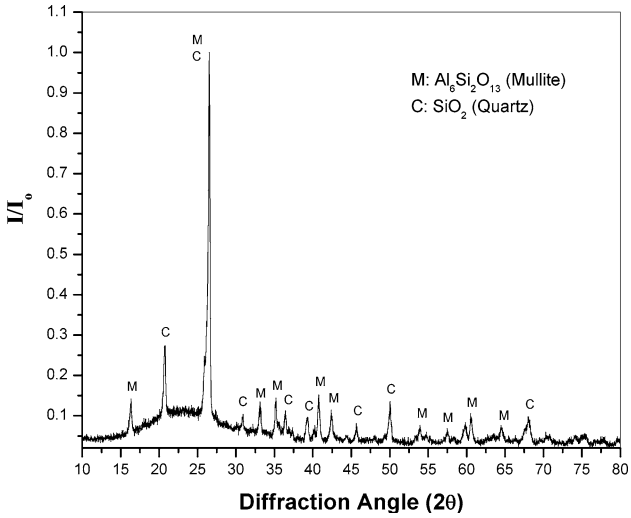

Fig. 4 X-ray diffraction pattern obtained from the FA

Table 3 Chemical composition of EAFD and FA fillers

Wt.%	Al	Ca	Fe	Mg	Pb	K	Si	Na	Ti	Mn	Zn	O
EAFD	2.05	1.47	21.33	3.70	2.08	0.23	3.20	2.27	...	4.77	38.51	15.39
FA	17.67	2.63	0.51	3.53	...	1.02	37.41	1.61	1.08	...	...	32.93

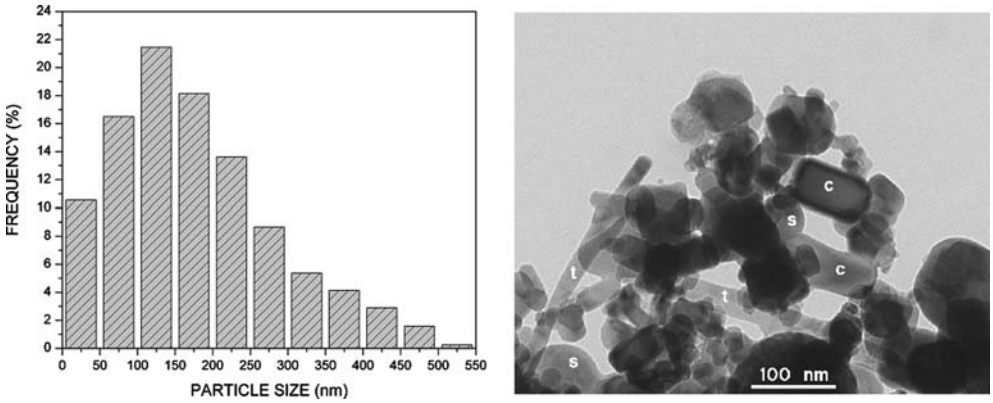

Fig. 3 Histogram and Bright field TEM image of the EAFD, morphology being indicated by spherical (*s*), faceted (*c*), and filamentary (*t*)

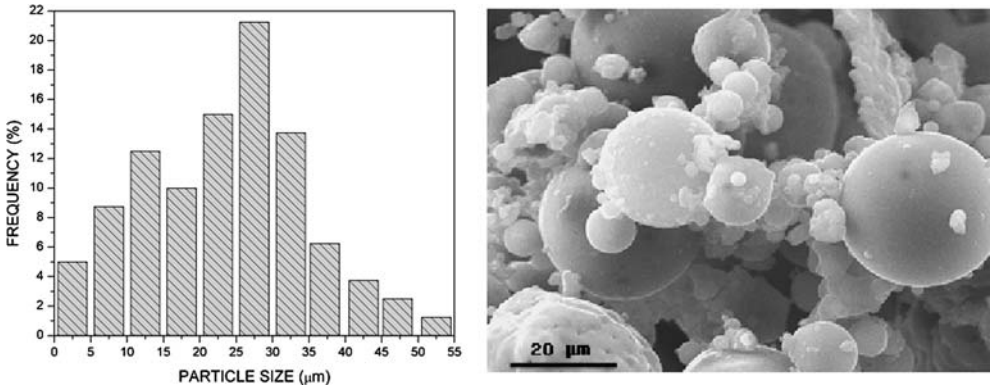

Fig. 5 Histogram and secondary electron SEM image of the FA

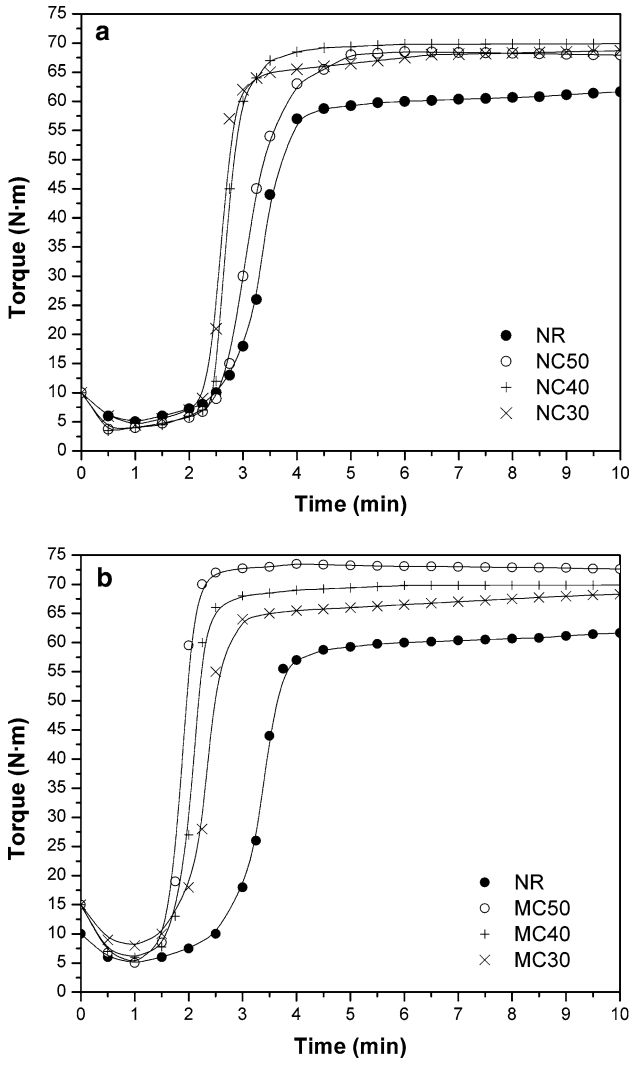

Fig. 6 (a) and (b) correspond to torque-time curves obtained from FA and EAFD filled natural rubber blends vulcanized at 160 °C

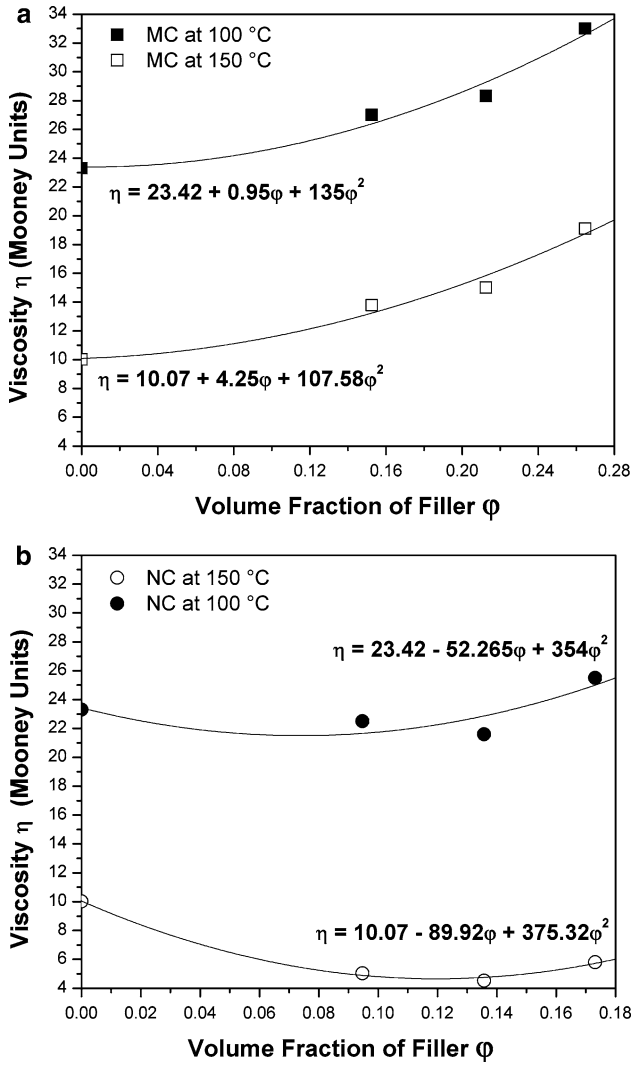

Fig. 7 Viscosity against the amount of filler incorporated in the rubber obtained at 100 and 150 °C. (a) Micrometric particles from FA, (b) nanometric particles from EAFD

Concerning to the properties of unvulcanized rubbers containing fillers, the viscosity follows the behavior of a suspension of spherical particles in a medium of viscosity η_o according to Guth's equation (Ref 14)

$$\eta = \eta_o(1 + \alpha_1\varphi_1 + \alpha_2\varphi^2) \quad \text{(Eq 1)}$$

where φ is the volume fraction of filler and the coefficients α_1, α_2 are just positive numerical factors. At a very small volume

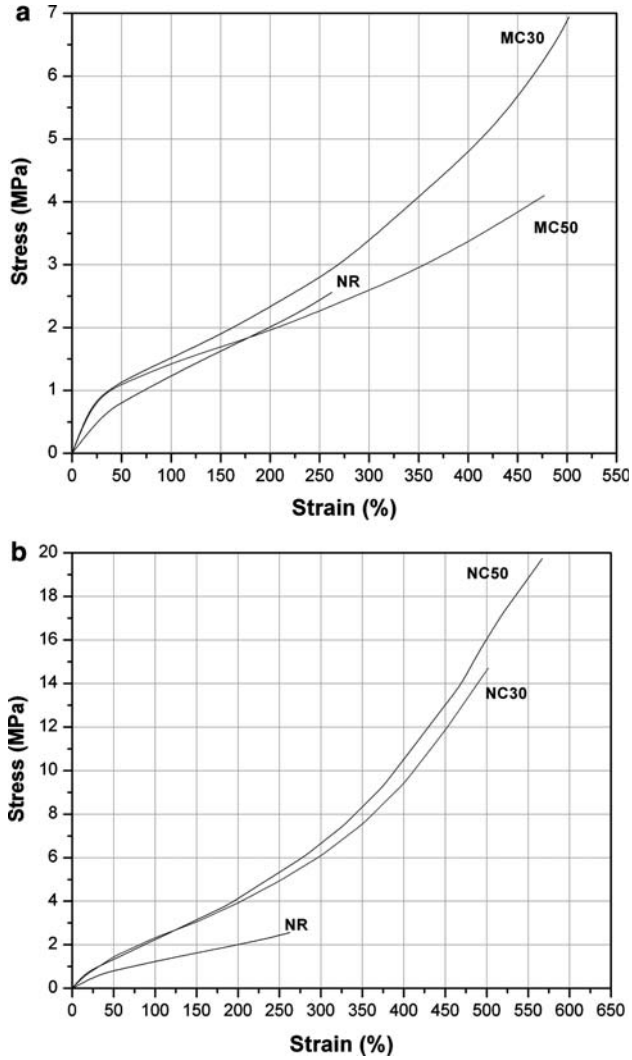

Fig. 8 Stress-strain curves of rubber composites reinforced with different amount of fillers. (a) Micrometric particles and (b) nanometric particles

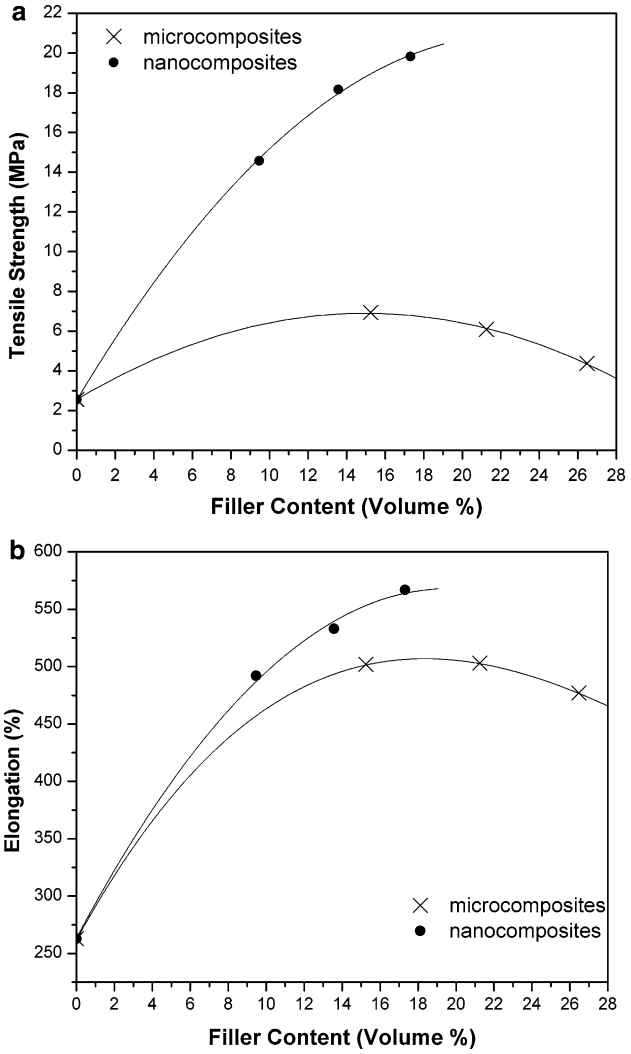

Fig. 9 Effect of the addition of filler content and particle size on mechanical properties of natural rubber composites. (a) Tensile strength and (b) deformation at break

fraction φ, the third term in the parentheses vanishes and the equation reduces to the familiar Einstein viscosity law (Ref 15).

Micrometric-size glass beads and medium thermal black (N990) obey Eq 1 rather well (Ref 16), while high-surface area fillers never do, but in both cases, higher filler content leads to higher viscosity. The reasons for this involves the mutual interaction of particles conforming the aggregates, so the medium cannot move freely through their internal void space and occluded rubber therein augments the effective filler concentration (Ref 17).

Curves of viscosity vs. volume fraction of filler given by Mooney viscometry at 100 and 150 °C are shown in Fig. 7 for each type of powder. Figure 7a shows for the micrometric particles a quadratic relationship between the volume fraction of filler in the rubber matrix and its viscosity, therefore obeying Eq 1 according to the parameters obtained from Fig. 7a. In contrast, Fig. 7b illustrates for the nanometric particles the occurrence of a zone where an increase of the filler content can lead to lower viscosity, afterwards the viscosity increase as filler content increase, disobeying Eq 1 according to the negative coefficient assigned to the linear term. At present there is no clear explanation to this effect, but probably the reason of this behavior could be related to the presence of particle agglomeration as shown in Fig. 2 together with the fact that $ZnFe_2O_4$ corresponds to a magnetic ceramic with spinel structure and will have saturation magnetizations determined by the substitution of nonmagnetic Zn^{2+} by Mn^{2+}, such as $Mn_{1-x}Zn_xFe_2O_4$ a widely used commercial ferrite (Ref 18). Consequently, at low-volume concentration, shear stresses are not high enough to break the agglomerates so the effective particle size is larger. Besides, probably there is a small magnetic interaction between the agglomerates, so slippage between rubber layers could be assisted, given a final effect of lower apparent viscosity. Nevertheless, further studies have to be performed in order to clarify the observed reduction on viscosity.

3.3 Mechanical Properties

It has been shown that the stress-strain curves for particle filled rubber systems are affected by the crosslink density of rubber matrix (Ref 19, 20), the size of agglomerates (Ref 21) and the rubber/particle interactions (Ref 6, 19). Considering that all rubber composites were processed in the same way so

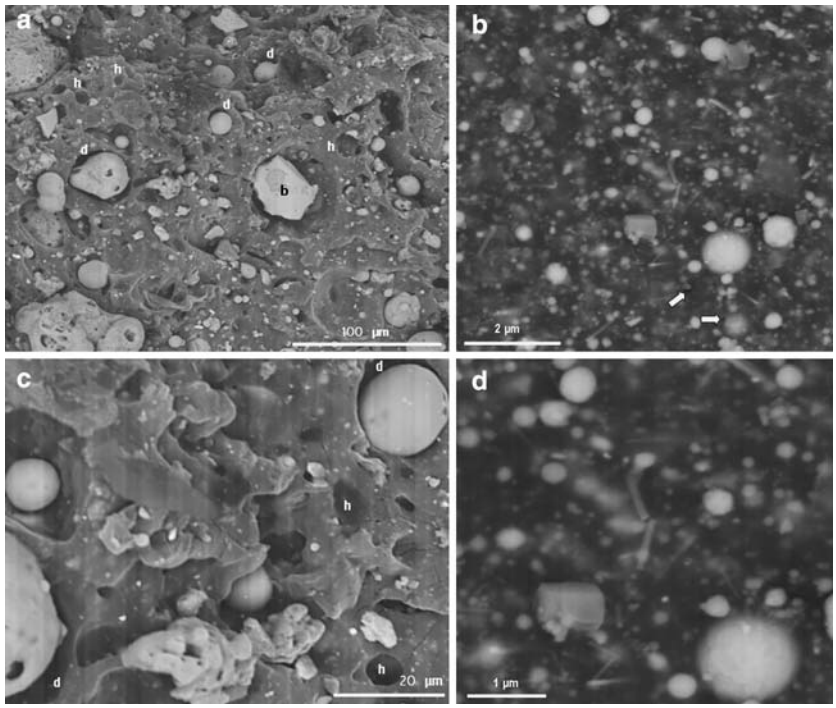

Fig. 10 Vulcanized rubber composite blended with: (a) and (c) MC30 corresponding to 12.25 vol.% of micrometric particles. (b) and (d) NC50 corresponding to 17.31 vol.% of nanometric particles. Arrows indicate holes or voids

the crosslink density of the rubber matrix was approximately the same in all samples, then any difference observed in mechanical properties between composites made from FA and EAFD powders should be related to the higher surface area of the nanometric particles.

For simplicity only five of the measured stress-strain curves obtained from the prepared rubber composites are presented in Fig. 8. As expected after the vulcanizing process, the micrometric composites exhibited a moderate increase in tensile strength (4-7 MPa) and elongation (≈500%) compared with vulcanized natural rubber (2.5 MPa and 250%), and the maximum values were attained at relative low-volume fractions of filler (Fig. 9). On the other hand, in relation to the nanometric particles Fig. 8 clearly suggests that there is an enhancement in tensile strength and elongation, reaching the vulcanized nanocomposites a tensile strength of almost 20 MPa and elongations up to 575%. Besides, the optimum volume content of nanometric particles that maximize the elongation and the tensile strength of the composite probably is situated between 22 and 26 vol.% (Fig. 9). Moreover, the tensile strength of the EAFD nanocomposites is equivalent to those of commercial NR/carbon black systems, where tensile strength usually range between 20 and 28 MPa (Ref 2).

Fractured surface of micro and nanometric reinforced rubbers were observed by SEM in order to know how particles were affected inside the composites together with the possible examination of rubber-particle bonding after the mechanical evaluation.

Figure 10 corresponds to the fractured surface of composites having 15.25 vol.% of micrometric particles and 17.31 vol.% of nanometric particles. In the microphotographs showing the fracture surface of sample MC30 at two different magnifications (Fig. 10a and c), it was found that the presence of micrometric particles still embedded in the rubber matrix. Besides, there were also broken particles (*b*) together with particles starting to be detached from the rubber matrix (*d*) and an important concentration of holes (*h*), probably where micrometric particles were embedded before fracture. On the other hand, the corresponding microphotographs of the fracture surface of sample NC50 at two different magnifications are shown in Fig. 10b and c. In this case, images indicated that nanometric particles are not fully exfoliated in the rubber matrix and fractured surfaces did not show a high concentration of defects like broken particles or detached particles as in the microcomposites, most likely as a consequence of nanometric size of the particles. Even so, some lack of defects probably could be associated to a certain extent to the characteristic low resolution of SEM techniques at high magnifications.

Another important parameter in rubber materials is its hardness, which is greatly determined by the type and amount of reinforcing filler used (Ref 16, 20). High structure, volume content, and amount of filler's surface available for attachment to the rubber should contribute to make the composite harder. Figure 11 introduces the dependence of the rubber composites hardness in terms of the type and amount of filler. Here, the hardness of the composites made of micrometric and nanometric particles presents a linear relationship with volume content, but micrometric made composites always having values lower than those observed on composites made with nanometric particles.

Experimental evidence has shown that debonding is delayed to higher and higher elongations when hardness increase (Ref 22, 23). Subsequently, the obtained stress-strain results together with hardness values and SEM images suggest that there is better bonding between nanometric particles and rubber

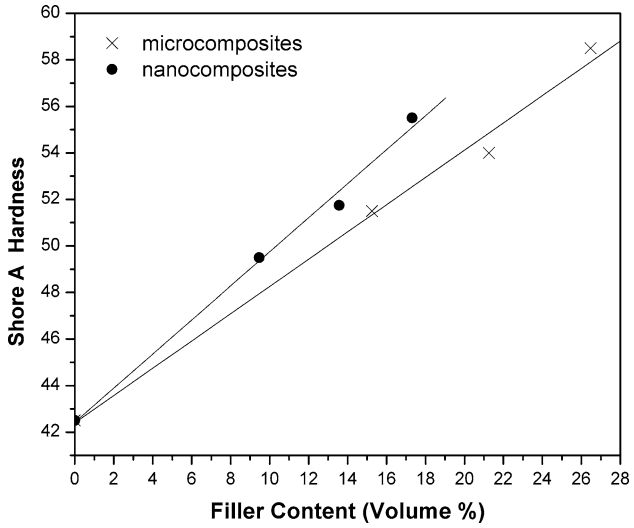

Fig. 11 Effect of the addition of filler content and particle size on hardness of natural rubber composites

matrix than their micrometric counterparts, giving a rubber base material having enhanced performance.

4. Conclusions

Nanometric particles obtained from EAFD were evaluated as possible reinforcement in natural rubber and compared with micrometric particles obtained from FA. Processing of rubber-$ZnFe_2O_4$ nanocomposites was evaluated and it was found that viscosity of rubber filled with micrometric particles obey the Guth's equation. In contrast, a non-linear behavior zone where viscosity decrease as filler content increase was observed with the nanometric $ZnFe_2O_4$. It was assumed that aggregates rupture jointly with magnetic interactions could be the origin of this behavior. Nevertheless, at present there is no experimental validation for a real rationalization of the observed behavior on the diminution of the viscosity of the unvulcanized rubber filled with $ZnFe_2O_4$ nanometric particles.

Concerning the mechanical properties of rubber-$ZnFe_2O_4$ nanocomposites, the effect of nanometric particles is to increase the hardness, elongation and tensile strength of vulcanized rubber composites obtained with this filler, suggesting a better rubber/filler interaction as result of the high-specific surface area. Moreover, the tensile strength of the EAFD nanocomposites is equivalent to those of commercial NR/carbon black systems, where tensile strength usually ranges between 20 and 28 MPa. Finally, the present results open the possibility for an industrial new and inexpensive reinforcement for natural rubber if the proper surface modifiers could be found to improve even more the final properties of the composites.

Acknowledgments

The authors acknowledge the support received from UASLP program FAI-C25-2001 and from the National Council for Science and Technology of Mexico (CONACyT) and DGAPA-UNAM project IN-107502.

References

1. Indian Rubber Institute, *Rubber Engineering*, McGraw-Hill Companies Inc., 2000
2. M. Morton, *Rubber Technology*, 3rd ed., Van Nostrand Reinhold, 1987
3. C. Furtado, R. Nunes, and F. Siqueira, SBR-Mica-Silica Compositions and their Physico-Mechanical Behavior, *Polym. Bull.*, 1995, **34**, p 627–633
4. W.C. Zuiderduin, C. Westzaan, J. Huetink, and R.J. Gaymans, Toughening of Polypropylene with Calcium Carbonate Particles, *Polymer*, 2003, **44**, p 261–275
5. J.E. Mark, B. Erman, and F.R. Eirich, *Science and Technology of Rubber*, 2nd ed., Academic Press Inc., 1994
6. M.P. Wagner, Reinforcing Silica and Silicates, *Rubber Chem. Technol.*, 1976, **49**, p 703–775
7. M.P. Wagner, Fine Particle Silica in Tire Treads, Carcass and Steel-Belt Skim, *Rubber Chem. Technol.*, 1977, **50**, p 356–363
8. S.S. Choi, Properties of Silica-Filled Styrene-Butadiene Rubber Compounds Containing Acrylonitrile-Butadiene Rubber, *J. Appl. Polym. Sci.*, 2002, **85**, p 385–391
9. Z. Wang and T.J. Pinnavaia, Nanolayer Reinforcement of Elastomeric Polyurethane, *Chem. Mater.*, 1998, **10**, p 3769–3771
10. A.R. Payne and R.E. Whittaker, Low Strain Dynamic Properties of Filled Rubbers, *Rubber Chem. Technol.*, 1971, **44**, p 440–459
11. M.J. Wang, The Role of Filler Networking in Dynamic Properties of Filled Rubber, *Rubber Chem. Technol.*, 1999, **72**, p 430–448
12. D. Schaefer and C. Chen, Structure Optimization in Colloidal Reinforcing Fillers: Precipitated Silica, *Rubber Chem. Technol.*, 2002, **75**, p 773–794
13. C.R. Herd, G.C. McDonald, and W.M. Hess, Morphology of Carbon-Black Aggregates: Fractal Versus Euclidean Geometry, *Rubber Chem. Technol.*, 1992, **65**, p 107–129
14. E. Guth, Theory of Filler Reinforcement, *J. Appl. Phys.*, 1945, **16**, p 20–28
15. L.E. Nielsen, *Polymer Rheology*, Marcel Dekker Inc., 1977
16. G. Kraus, Interaction of Elastomers and Reinforcing Fillers, *Rubber Chem. Technol.*, 1965, **38**, p 1070–1114
17. A.I. Medalia, Filler Aggregates and their Effect on Reinforcement, *Rubber Chem. Technol.*, 1974, **47**, p 411–433
18. R.C. O'Handley, *Modern Magnetic Materials: Principles and Applications*, John Wiley & Sons Inc., 2000
19. F. Yatsuyanagi, N. Suzuki, M. Ito, and H. Kaidou, Effects of Surface Chemistry of Silica Particles on the Mechanical Properties of Silica Filled Styrene-Butadiene Rubbers, *Polym. J.*, 2002, **34**, p 332–339
20. L.E. Nielsen, and R.F. Landel, *Mechanical Properties of Polymers and Composites*, 2nd ed., Marcel Dekker, 1994
21. N. Suzuki, F. Yatsuyanagi, M. Ito, and H. Kaidou, Effects of Surface Chemistry of Silica Particles on Secondary Structure and Tensile Properties of Silica-Filled Rubber Systems, *J. Appl. Polym. Sci.*, 2002, **86**, p 1622–1629
22. E. M. Dannenberg and J.J. Brennan, Strain Energy as a Criterion for Stress Softening in Carbon-Black-Filled Vulcanizates, *Rubber Chem. Technol.*, 1966, **39**, p 597–608
23. S. Rios, R. Chicurel, and L.F. del Castillo, Potential of Particle and Fiber Reinforcement of Tire Tread Elastomers, *Mater. Design.*, 2001, **22**, p 369–372